

Megascience Projects at the Brookhaven National Laboratory

G Nigmatkulov

National Research Nuclear University MEPhI (Moscow Engineering Physics Institute),
Moscow, 115409, Russia

E-mail: ganigmatkulov@mephi.ru

Abstract. Brookhaven National Laboratory (BNL) is a multipurpose research center that primarily supported by the U.S. Department of Energy (DOE) Office of Science. BNL operates cutting-edge large-scale facilities for studies in physics, chemistry, biology, medicine, applied science, and a wide range of advanced technologies. Relativistic Heavy Ion Collider (RHIC) is a megascience facility at BNL that allows to conduct research in nuclear and particle physics. In these proceedings, we will review the current status and future prospects of the megascience complex RHIC.

1. Introduction

In 1970s, after the quark model and Quantum Chromodynamics (QCD) were introduced, it was suggested that the matter consisting of quarks and gluons, called Quark-Gluon Plasma (QGP), may exist [1–5]. The QGP was introduced as a dilute gas (plasma) of weakly coupled partons. This scenario could work at high temperatures. A few years before the fundamental theory of the strong interaction between quarks and gluons known as quantum chromodynamics (QCD) was founded, R. Hagedorn theoretically shown [6] that hadronic matter features a phase boundary at lower temperature, $T(H) = 170$ MeV. These results inspired the nuclear and particle physics community to explore the possibility to create and study QGP by colliding heavy ions at high energy.

The QCD predicts [7,8] a phase transition to occur between deconfined quarks and confined hadrons. The main goals of the relativistic heavy ion physics is to determine the phase diagram for matter that interacts via the strong nuclear force (Fig. 1), learn QCD matter properties, and get information about the nature of the deconfined QGP phase. The most experimentally accessible way to characterize the QCD phase diagram is in the plane of temperature (T) and the baryon chemical potential (μ_B).

A scan across beam energies is used to investigate the QCD phase structure as a function of T and μ_B . A number of experiments were carried out at AGS (BNL) at $2 < \sqrt{s_{NN}} < 6$ GeV, SPS (CERN) up to about $\sqrt{s_{NN}} \approx 20$ GeV, RHIC (BNL) up to 200 GeV, and LHC (CERN) up to 5.02 TeV. The first phase of the Beam Energy Scan program (BES-I) and the top energy at RHIC has allowed access to a region of the QCD phase diagram covering a range of baryochemical potential (μ_B) from 20 to 420 MeV corresponding to Au+Au collision energies from $\sqrt{s_{NN}} = 200$ to 7.7 GeV, respectively.

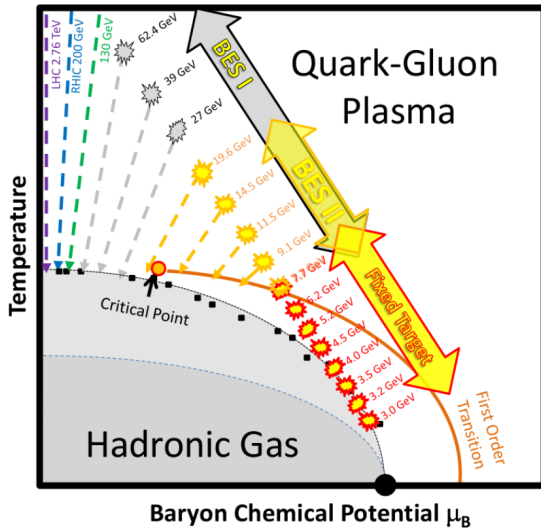


Figure 1. (Color online) QCD phase diagram.

2. Highlights from the STAR program

The STAR collaboration has conducted a series of correlation measurements over the last few years in order to gain a better understanding of the QCD phase diagram and the bulk characteristics of the QGP phase. Some STAR studies on bulk correlations are highlighted here, and they are expected to provide light on the QCD phase diagram as well as the QGP transport properties. For more detailed reviews see Refs. [9–12] and references therein.

2.1. Net-proton number fluctuations

One of the major purposes of the STAR Beam Energy Scan (BES) program is to look for probable indications of the QCD critical point (CP) by altering the collision energy and scanning the T and μ_B plane. The correlation length diverges when the system formed in heavy ion collisions approaches the CP. Higher order cumulants of conserved net-particle multiplicity distributions are sensitive to such correlation lengths [13] because more fluctuations in the net-particle multiplicity distributions result from the divergence in correlation length.

It has been predicted that the ratios of the cumulants of identified net-particle multiplicity distributions, such as net-protons, are ideal observables sensitive to the onset of the QCD phase transition and the vicinity of the CP. A non-monotonic fluctuation of these cumulant ratios as a function of collision energy, such as C_4/C_2 (also denoted as $\kappa\sigma^2$), has been proposed as an experimental signature of the CP.

Using cumulant ratios has the advantage of canceling volume fluctuations to first order. Furthermore, these cumulant ratios are connected to the baryon-number susceptibilities ratio at a particular T and μ_B . At the vicinity of CP, QCD-based calculations predict non-Gaussian net-baryon number distributions and diverging susceptibilities, resulting in non-monotonic change in these ratios as a function of collision energy.

Figure 2 shows the collision energy fluctuation of net-proton $\kappa\sigma^2$ (protons and antiprotons are selected within the acceptance of $0.4 < p_T < 2.0$ GeV/c and $|y| < 0.5$) for central and peripheral Au+Au collisions [14, 15].

A non-monotonic behaviour with beam energy is seen for $\kappa\sigma^2$ with a significance of 3.0 in central Au+Au collisions. The results obtained by statistical hadron gas (HRG) and a nuclear transport without a critical point (UrQMD) models show monotonic behavior with beam energy in peripheral collisions.

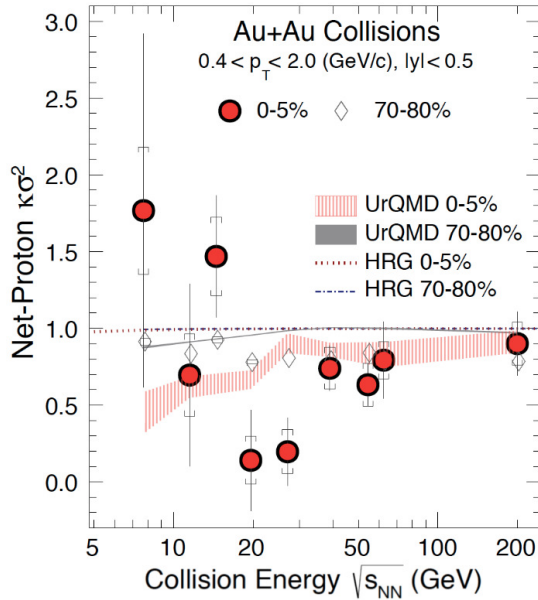


Figure 2. (Color online) The $\kappa\sigma^2$ as a function of collision energy for net-proton distributions measured in central (0-5%) and peripheral (70-80%) Au+Au collisions within $0.4 < p_T < 2.0$ GeV/c and $|y| < 0.5$. Statistical and systematic uncertainties are represented by the error bars and caps, respectively. Results from a hadron resonance gas (HRG) model are represented by the dashed and dashed-dotted lines. The shaded bands represent the results of a transport model calculations (UrQMD).

2.2. Anisotropic flow

The azimuthal distribution of soft particles emission is not isotropic in relativistic heavy-ion collisions. Fourier coefficients (v_n) can be used to describe measurements of these anisotropies in relation to so-called flow symmetry planes (v_n):

$$\frac{dN}{d\phi} \propto 1 + 2 \sum_{n=1}^{\infty} v_n \cos[n(\phi - \Psi_n)], \quad (1)$$

where ϕ is an azimuthal angle of a produced particle, and Ψ_n is an azimuthal angle of the n^{th} -order event plane [16]. Values of v_n as a function of collision energy, centrality, particle species, and transverse momentum provide important information on the system's shear and bulk viscosities, as well as some insight into the relevance of initial-state fluctuations in the development of the QGP.

Figure 3 shows the $\sqrt{s_{NN}}$ dependence of $v_2(p_T)$ and $v_3(p_T)$ for identified particles (π^\pm , K^\pm , p , \bar{p}) for 0-60% collision centrality.

The left plot of this figure shows results for positive particles and the right shows the same for negative particles. The charged pion π^+ and π^- $v_2(p_T)$ values have almost comparable shapes and amplitudes at higher energies of 27, 39, and 62.4 GeV that is expected for the particles with the same mass and number of quarks. At lower energies, the difference between $v_2(\pi^+)$ and $v_2(\pi^-)$ grows with $v_2(\pi^-)$ being greater than $v_2(\pi^+)$ for all p_T values. The $v_2(\pi^-)$ may be greater than $v_2(\pi^+)$ because of the Coulomb repulsion of π^+ by the midrapidity protons or due to the chiral magnetic effect in finite baryon density matter formed in heavy-ion collisions [17]. The triangular flow of particles is sensitive to the event-by-event fluctuations of initial geometry. Values of triangular flow v_3 are multiplied by 2.5 to improve visibility. It is seen that triangular

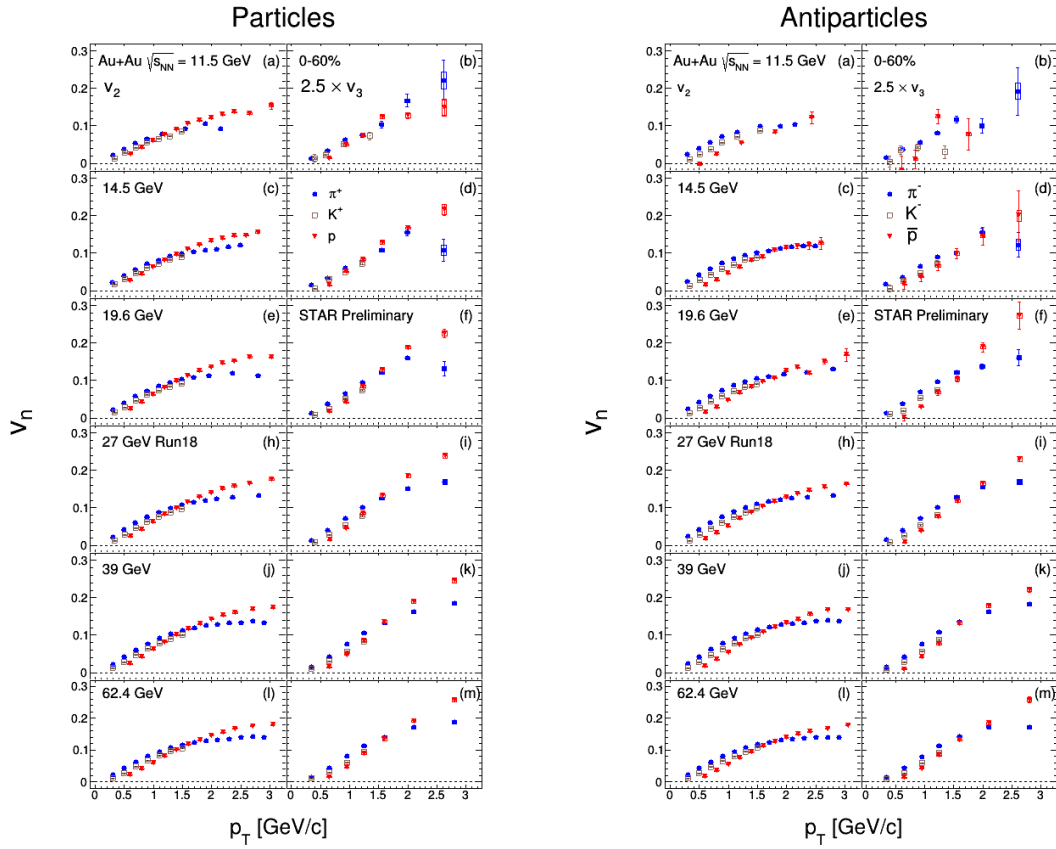


Figure 3. (Color online) Elliptic and triangular flow of π^+ , K^+ , p (left) and π^- , K^- , \bar{p} (right) for 0-60% centrality and six collision energies.

flow values have mass ordering at low p_T range less than $1.5 \text{ GeV}/c$ and meson/baryon splitting for transverse momentum greater than $2 \text{ GeV}/c$. The v_3 weakly depends on the collision energy.

2.3. Correlation femtoscopy

In high-energy heavy-ion collisions, the correlation femtoscopy technique may be utilized to assess the spatial and temporal extents of the particle-emitting region. The extracted from the analysis femtoscopy radii represent collective effects in a variety of ways most notably in their dependence on the transverse pair momentum [18–22]. One way for examining the particle production process is to measure the spatial and temporal scales of the particle-emitting source. In small systems such as $p+\text{Au}$ and $d+\text{Au}$ may depend on the initial conditions [23, 24].

The identical pion femtoscopy analysis has been performed at $\sqrt{s_{NN}} = 200 \text{ GeV}$ in $p+\text{Au}$ and $d+\text{Au}$ collisions at STAR. Only tracks selected within the momentum range $0.15 < p < 0.8 \text{ GeV}/c$ and pseudorapidity range $|\eta| < 0.5$ were used in the analysis. Pions were identified by specific ionization energy losses in TPC. The dependence of the invariant radii on the transverse momentum of the pairs ($k_T = (p_{1,T} + p_{2,T})/2$), where $p_{1,T}$ and $p_{2,T}$ are the transverse momenta of the first and second particle from the pair, is investigated to explore the space-time structure of the pion emission source in $p+\text{Au}$ and $d+\text{Au}$ collision systems.

The charged pion invariant radii dependence on k_T is shown in Fig. 4.

Pion femtoscopy radii decrease with k_T that suggests the presence of collective radial flow in small collision systems. The sizes of the particle emission region are larger for $d+\text{Au}$ collisions than that for $p+\text{Au}$ collisions at $k_T < 0.5 \text{ GeV}/c$.

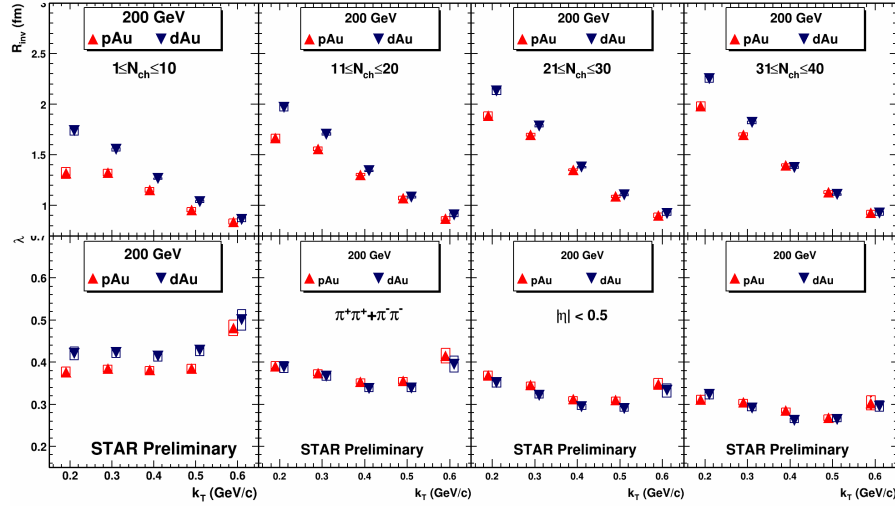


Figure 4. (Color online) Dependence of identical charged pion invariant radii (top row) and correlation strength parameter (bottom row) on k_T and multiplicity for p+Au and d+Au collisions at $\sqrt{s_{NN}} = 200$ GeV. Statistical and systematic uncertainties are shown by vertical lines and boxes, respectively.

2.4. Global hyperon polarization

In non-central collisions, relativistic hydrodynamics predicts that QGP will have a lot of vorticity. It manifests as polarization of generated particles along the orbital angular momentum of the system. Because of the spin-orbit coupling, the generated particles will have a global spin polarization in the direction of the system angular momentum. The parity violating weak decays allows to use hyperons in order to measure the so-called global polarization. In hyperon weak decays the angular distribution of daughter baryons in the parent hyperon rest frame can be described as:

$$\frac{dN}{d \cos \theta^*} \propto 1 + \alpha_H P_H \cos \theta^*, \quad (2)$$

where α_H is the hyperon decay parameter, P_H is the hyperon polarization, and $\cos \theta^*$ is the angle between the polarization vector and daughter baryon momentum in the hyperon rest frame [25]. Global polarization value can be obtained by measuring daughter baryon's momentum projection on initial angular momentum direction. One can measure it in respect to reaction plane

Figure 5 shows the global polarization of $\Lambda + \bar{\Lambda}$ and $\Xi^- + \bar{\Xi}^+$ hyperons as a function of collision energy for the centrality bin 20-50% (20-80% for $\Xi^- + \bar{\Xi}^+$ at $\sqrt{s_{NN}} = 200$ GeV due to smaller signal).

At top RHIC energy ($\sqrt{s_{NN}} = 200$ GeV) no significant difference between Λ and $\bar{\Lambda}$ polarization within the uncertainties [26]. Global hyperon polarization decreases with increasing collision energy. The Ξ global polarization was measured using two methods: 1) directly via the angle of daughter Λ , and 2) via its Λ daughter decays. Both measurements are consistent within given large uncertainties. Within uncertainties it is also consistent with Λ global polarization.

3. Beam Energy Scan II

Physicists achieved a goal of smashing ions at the lowest and most challenging energy in a 21st run at the Relativistic Heavy Ion Collider (RHIC), a US Department of Energy (DOE) user facility for nuclear physics research at Brookhaven National Laboratory. The STAR experiment also finished the planned data taking ahead of time.

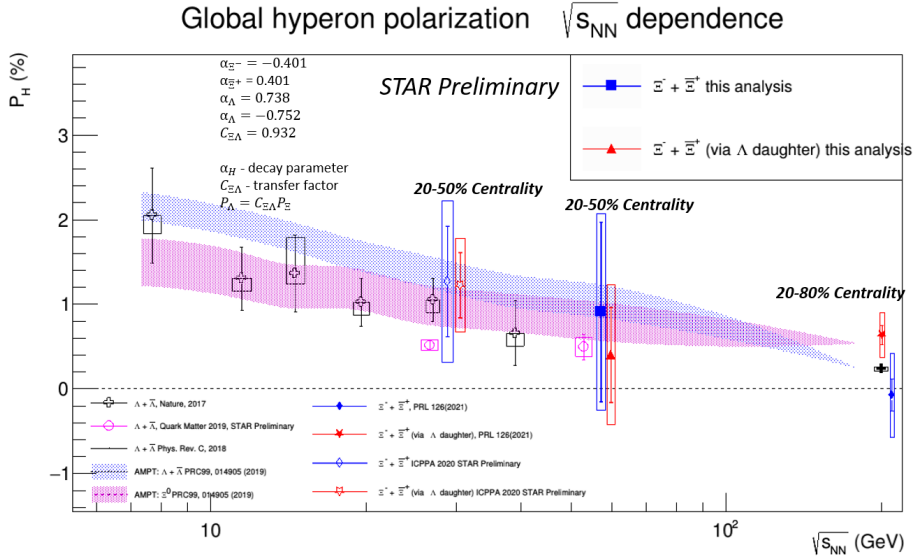


Figure 5. (Color online) Global polarization of $\Lambda + \bar{\Lambda}$ and $\Xi^- + \bar{\Xi}^+$ as a function of collision energy for 20-50% central Au+Au collisions.

As RHIC enters the last years of its experimental program, an early completion of the final phase of Beam Energy Scan II (BES-II) allowed STAR to collect critical new data. After the RHIC physics program is completed, some of the RHIC accelerator core components will be utilized to build the Electron-Ion Collider, a new nuclear physics research facility (EIC).

Scientists finished the last step of BES-II, a three-year investigation of what occurs when gold ions (gold atoms stripped of their electrons) collide at different energies. At 3.85 billion electron volts (GeV) per nucleon (proton or neutron), the experiment successfully acquired information about collisions. Data from fixed-target runs at 44.5, 70, and 100 GeV/nucleon were also successfully gathered.

It is challenging to deliver intense colliding ion beams at low energies. The lesser the energy, the more difficult it is to preserve the beam quality. RHIC operations were controlled by scientists from the Collider-Accelerator Department (C-AD), who developed a first-of-its-kind beam-cooling technology to take advantage of Run 21. In 2020 and 2021 RHIC run demonstrated the world's first application of electron cooling in a collider, when the Low Energy RHIC electron Cooling (LEReC) system ran at full capacity for the first time. To remove part of the heat from the accelerated ions, the system injects cool electron beams into the stream. This cooling helps to keep the ions compact and more likely to collide by preventing them from spreading out.

In 2021 the usage of LEReC was even more critical for the lowest-of-low collision energies. The accelerator developments made before and during the run increased the likelihood of collisions when the beams intersected near the center of the STAR detector.

The data gathered by the STAR experiment during this run might be crucial in the searching for evidence of the “critical point” in the transition of nuclear matter to a soup of free quarks and gluons known as a quark-gluon plasma (QGP). This critical point affects the transition between the two phases of matter.

4. Beyond the BES-II

4.1. O+O collisions

The hydrodynamic response of a fluid-like system to geometric shape fluctuations in the initial state has been satisfactorily described for collective long-range azimuthal correlations in A+A

collisions. Observations of comparable collective effects in small-system collisions, such as pp and p+A collisions, have attracted interest in the community. The interpretation of a fluid-like state that emerged there has been questioned, since the small system size and lifetime may preclude it from thermalizing and evolving hydrodynamically. Instead, collectivity emerging from early momentum correlations driven by gluon saturation models [27] or a few scatterings among partons (without hydrodynamization) [28,29] have been presented as an alternate sources of collectivity that might be dominant in small systems.

After BES-II was completed, the beam time was allocated to outlined additional priorities in the planned beam user request for Run 21. Collisions between oxygen ions were recorded as additional priority for Run 21. Experiments at RHIC have involved collisions of a variety of heavy ions with other heavy ions, heavy with light, and intermediate elements. For the RHIC program, oxygen-on-oxygen collisions are a novel species combination. These data will help to understand the early-time conditions of small systems and allow for a direct comparison with a similarly proposed higher-energy O+O run at the LHC, and would strengthen the case for a small system scan as a supplement to the NA61/SHINE collaboration's ongoing efforts at SPS energies, as well as other proposed light-ion species at the LHC.

4.2. Spin physics

The STAR Cold QCD program aims to investigate the spin and flavor structure of a proton, as well as the role of spin in QCD. To do it, STAR utilizes a RHIC's unique capability to deliver longitudinally and transversely polarized p+p and p+A collisions at several energies. Longitudinal beam polarization measurements have offered fresh insights into the helicity structure of a proton, while transverse polarization measurements have provided new options to explore polarized parton distribution functions (PDFs) in the collinear and transverse momentum dependent frameworks. Furthermore, the unpolarized p+p collision cross section measurements provide important information for constraining collinear and transverse momentum dependent unpolarized PDFs.

Run 22 will make full use of STAR's enhanced forward detection capabilities, which include a new Forward Calorimeter System (FCS) and Forward Tracking System (FTS) positioned between $2.5 < \eta < 4$, as well as the recently upgraded BES-II detectors. These data will allow STAR to investigate forward jet physics in both the high-x (mainly valence quark) and low-x (primarily gluon) partonic regimes with high accuracy.

5. Future facilities

5.1. sPHENIX

sPHENIX is a proposal for a large improvement to the RHIC-based PHENIX experiment, capable of measuring jets, jet correlations, and Upsilon in order to estimate the temperature dependence of QGP transport coefficients [30]. The temperature scales at RHIC and LHC allow to create an intrinsically non-perturbative system. The variation in the initial temperature formed in RHIC and LHC collisions is thought to be linked to differences in the nature of the QGP. In order to correctly define the new QGP state of matter, such changes in the system's attributes must be determined. Furthermore, much more research is needed to understand the many-body collective effects in the QGP. A new detector sPHENIX is under construction in the old PHENIX hall and is expected to take data in 2023–25.

5.2. EIC

RHIC will have a major upgrade and will be turned to the Electron-Ion Collider (EIC) with the addition of a high intensity electron beam facility. At least one new detector will have to be built to study the collisions [31]. The EIC will be the most powerful electron microscope ever created to investigate protons, neutrons, and atomic nuclei. The EIC is capable of colliding

polarized electron beams with polarized light ion beams at high intensity. Brookhaven National Laboratory (BNL) and the Thomas Jefferson National Accelerator Facility (JLab) in Newport News, Virginia are working together to build the EIC. It will bring together physicists and engineers from across the world, as well as from other laboratories and institutions in the United States. This will take a decade to complete, with beam operations beginning in the early 2030s. EIC is aiming to answer next key scientific questions: 1) How can partons and their underlying interactions give rise to nucleonic characteristics like mass and spin? 2) How are partons distributed in both momentum and coordinate space inside the nucleon? 3) What is the interaction of color-charged quarks, gluons, and jets with a nuclear medium? How can these quarks and gluons give rise to confined hadronic states? 4) How do the interactions between quarks and gluons result in nuclear binding? 5) What effect does a dense nuclear environment have on quark and gluon dynamics, correlations, and interactions? The EIC covers a center-of-mass energy range for e+p collisions of \sqrt{s} of 20 to 140 GeV.

6. Summary

A short review of the experiments and results from the megascience complex RHIC was presented. By the middle of 2021 the Hot QCD program has been successfully finished. During the Beam Energy Scan II and Fixed-target programs, the STAR experiment took many datasets in the collision energy range $\sqrt{s_{NN}} = 3\text{-}27$ GeV. The program required to fulfil the upgrade of the accelerator - bunched electron beam cooling. Some selected results from the BES-II program have been presented and physics implications have been discussed. Next years of RHIC operations will include the STAR taking data to study the proton spin structure and installation a newcomer sPHENIX experiment. A transition from RHIC to EIC has been discussed.

Acknowledgments

The work was supported by the Ministry of Science and Higher Education of the Russian Federation, Project “Fundamental properties of elementary particles and cosmology” No 0723-2020-0041 and by the National Research Nuclear University MEPhI within the Program “Priority-2030”.

References

- [1] Collins J C, Perry M J 1975 *Phys. Rev. Lett.* **34** 1353
- [2] Cabibbo N, Parisi G. 1975 *Phys. Lett. B* **59** 67
- [3] Shuryak E V 1978 *JETP* **47** 212
- [4] Shuryak E 1980 *Phys. Rep.* **61** 71
- [5] McLerran L 1988 *Rev. Mod. Phys.* **58** 1021
- [6] Hagedorn R 1965 *Suppl. Nuovo Cim.* **3** 147
- [7] Aoki Y, Endrodi G, Fodor Z. *et al.* 2006 *Nature* **443** 675
- [8] Cheng M, Christ N, Datta S *et al.* 2008 *Phys. Rev. D* **77** 014511
- [9] Nigmatkulov G 2020 *J. Phys.: Conf. Series* **1685** 012022
- [10] Nigmatkulov G 2019 *J. Phys.: Conf. Series* **1390** 012020
- [11] Nigmatkulov G 2019 *EPJ Web Conf.* **222** 01004
- [12] Nigmatkulov G 2019 *EPJ Web Conf.* **204** 03010
- [13] Hatta Y, Stephanov M A 2003 *Phys. Rev. Lett.* **91** 102003
- [14] Adam J *et al* 2021 *Phys. Rev. Lett.* **126** 092301
- [15] Abdallah M *et al* 2021 *Phys. Rev. C* **104** 024902
- [16] Voloshin S and Zhang Y 1996 *Z. Phys. C* **70** 665
- [17] Burnier Y *et al* 2011 *Phys. Rev. Lett.* **107** 052303
- [18] Semenova V K, Khyzhniak E V and Nigmatkulov G A 2019 *J. Phys.: Conf. Series* **1390** 012028
- [19] Ermakov N and Nigmatkulov G 2017 *J. Phys.: Conf. Series* **798** 012055
- [20] Kravchenko Y V *et al* 2021 *Phys. Scr.* **96** 104002
- [21] Kuzina E *et al* 2020 *J. Phys.: Conf. Series* **1690** 012131
- [22] Shapoval V M, Sinyukov Yu M 2021 *Nucl. Phys. A* **1016** 122322

- [23] Bzdak A *et al* 2013 *Phys. Rev. C* **87** 10
- [24] Plumberg C 2020 *Phys. Rev. C* **102** 054908
- [25] Voloshin S A, Niida T 2016 *Phys. Rev. C* **94** 021901
- [26] Adam J *et al* 2018 *Phys. Rev. C* **98** 14910
- [27] Dusling K *et al* 2016 *Int. J. Mod. Phys. E* **25** 1630002
- [28] He L *et al* 2016 *Phys. Lett. B* **753** 506
- [29] Romatschke P 2018 *Eur. Phys. J. C* **78** 636
- [30] Adare A *et al* 2014 arXiv:1501.06197
- [31] Deshpande A, Milner R, Venugopalan R and Vogelsang W 2005 *Ann. Rev. Nucl. and Part. Sci.* **55** 165